Sustainable Water Resources Management (2023) 9:162
https://doi.org/10.1007/s40899-023-00946-8

ORIGINAL ARTICLE

Geochemical simulation to assess the rock–water interaction in crystalline aquifers in São Paulo State, Southeastern Brazil

Elias Hideo Teramoto[1,2] · **Marcia Regina Stradioto**[1,2] · **Hung Kiang Chang**[1,2,3]

Received: 23 February 2023 / Accepted: 29 August 2023 / Published online: 14 September 2023

Abstract

The mechanisms underlying rock–water interactions play a crucial role in understanding groundwater quality. In this study, we examined hydrochemical data from 96 samples obtained from the crystalline aquifer system in the Southeast region of São Paulo State, Brazil, to characterize the hydrochemistry of these aquifers. Through the analysis of these data, we conducted several geochemical simulations to reproduce the hydrochemistry of the evaluated samples. Our analysis revealed two distinct evolutionary trends in hydrochemistry. The calcium–magnesium bicarbonate types can be attributed to the dissolution of amphiboles, while the sodium bicarbonate type can be reproduced by the dissolution of plagioclases. Contrary to the initial assumptions, the hydrochemistry of the evaluated samples does not mimic the mineralogy of the granitic/gneiss rocks. Instead, the cations dissolved in groundwater mainly originate from unstable and reactive minerals, primarily represented by amphiboles and plagioclases. Furthermore, considering that HCO_3^- is the primary species generated through silicate hydrolysis in an open system with respect to CO_2, we have developed a model that utilizes the concentration of this ion as a parameter to estimate the mass of rock involved in the rock–water interaction process. This model allows us to assess the extent of rock–water interaction based on HCO_3^- concentration. However, this approach is only valid in cases where additional sources of HCO_3^- are absent, and elevated PCO_2 levels prevent an increase in pH and carbonate precipitation. Overall, our findings make significant contributions to the comprehension of rock–water interaction processes and the assessment of groundwater quality in crystalline aquifers. However, they challenge the prevalent belief that the hydrochemistry of crystalline aquifers closely mirrors that of the fissured rocks through which groundwater flows.

Keywords Mineral water · Rock–water interaction · Silicate dissolution · Crystalline basement

Introduction

Crystalline aquifers are composed of hard rocks through which groundwater flows and is stored in fissures formed by various processes, including weathering, tectonics, thermal stress, and unloading (e.g., Lachassagne et al. 2021; Duranel et al. 2021; Yuguchi et al. 2021; Mao et al. 2022). Groundwater that fills these fissures undergoes complex chemical interactions with the host rock, known as rock–water interaction processes. The progression of rock–water interaction begins with groundwater recharge, which involves the input of low-ionic solutes that circulate through the interconnected network of rock fissures into the aquifers, gradually altering their initial composition (e.g., Almeida et al. 2022; Akurugu et al. 2022; Zango et al. 2023).

Chemical interactions between rock and water involve various distinct processes, such as dissolution/precipitation, ion exchange, oxidation, and reduction (e.g., Adabanija et al. 2020; Kumar and Kumar 2020; Fuoco et al. 2022; Ju et al. 2023; Mizuno et al. 2023). However, the dominant mechanism is undoubtedly represented by silicate hydrolysis (e.g., Banks and Frengstad 2006; Elango and Kannan 2007; Teramoto et al. 2019; Fuoco et al. 2022; Ghalit et al. 2023).

Numerous studies have investigated the evolution of hydrochemistry in groundwater stored in fractured rock,

✉ Elias Hideo Teramoto
elias.hideo-teramoto@unesp.br

[1] Centre of Environmental Studies (CEA), São Paulo State University, Campus of Rio Claro, Rio Claro, São Paulo, Brazil

[2] Laboratory of Basin Studies (Lebac), São Paulo State University, Campus of Rio Claro, Rio Claro, São Paulo, Brazil

[3] Departamento of Geology, São Paulo State University, Campus of Rio Claro, Rio Claro, São Paulo, Brazil

particularly focusing on incongruent silicate dissolution (e.g., Warnner et al. 2017; Sunkari and Abu 2019; Rashid et al. 2020; Abbas et al. 2021; Kouser et al. 2022; Cho and Choo 2019; Nakayama et al. 2022). The quantitative relationship between the progress of rock–water interaction and water quality in crystalline aquifers were explored in several previous works (e.g., Sung et al. 2012; Olofinlade et al. 2018; Ackerer et al. 2021; Roy et al. 2020; Choi et al. 2020; Ojoki et al. 2021; Fuoco et al. 2022). Furthermore, rock–water interaction also leads to the precipitation of new mineral phases, primarily clay minerals such as kaolinite, chlorite, and illite, while more stable phases like K-feldspar, quartz, and zircon accumulate as residual minerals (Procházka et al. 2018).

An essential aspect of rock–water interaction is comprehending the potential release of chemical species that may pose risks to human health. A prominent example is the fluoride ion (F^-), which is predominantly released into water through rock–water interaction, rendering it unsuitable for consumption. Numerous previous studies have reported the loss of potability resulting from the release of fluoride due to rock–water interaction in crystalline aquifers worldwide (e.g., Pauwels et al. 2015; Nagaraju et al. 2016; Martins et al. 2018; Sunkari and Abu 2019; Rashid et al. 2020; Cuccuru et al. 2020; Nakayama et al. 2022; Fuoco et al. 2022).

In addition to evaluating water quality, understanding rock–water interaction is also relevant for elucidating the dynamics of groundwater movement within bedrock fissures (e.g., Jaunat et al. 2012; Mao et al. 2022; Stober et al. 2022). For instance, dissolved silica derived from rock–water interaction can serve as a reliable indicator for estimating residence time in the crystalline aquifer (Benettin et al. 2015; Marçais et al. 2018; Mao et al. 2022). Furthermore, experimental data demonstrate that rock–water interaction can strongly impact the natural permeability of fissured rocks. It can increase permeability through the dissolution of certain minerals or decrease it through the precipitation of clay minerals along fractures (Sanchez-Roa et al. 2021).

One of the challenges in studying rock–water interaction is measuring the extent of this interaction, as only a few metrics have been proposed for its assessment. For example, Wanner et al. (2017) propose the use of Li as a proxy to determine the degree of interaction between water and rock, while Négrel (2006) suggests utilizing Sr, Ne, and rare-earth elements to quantify rock–water interaction. The quantification of rock–water interaction remains an ongoing issue, as different approaches and indicators provide valuable insights into this complex process. Wanner et al. (2017) propose the use of Li as a proxy, recognizing its potential in indicating the degree of interaction between water and rock. In contrast, Négrel (2006) suggests incorporating Sr, Ne, and rare-earth elements as alternative indicators for quantifying rock–water interaction.

As an alternative to simple metrics for estimating the extent of rock–water interaction, the application of geochemical modeling can provide quantitative and robust results, taking into account the complex interactions between various reactions (e.gAppelo and Postma 2004; Stradioto et al. 2020; Milesi et al. 2023). Geochemical modeling enables us to assess the coherence of anticipated dominant reactions and offers quantitative insights into the interaction between rocks and groundwater. It also facilitates establishing a connection between the evolution of groundwater hydrochemistry and the advancement of the rock–water interaction process. Despite the capabilities of geochemical models, only a limited number of studies have effectively employed them to replicate the water quality resulting from the interaction between groundwater and rock in crystalline aquifers, considering various reaction pathways (e.g., Fuoco et al. 2022; Manu et al. 2023).

The Precambrian crystalline basement outcrop and crystalline aquifers in São Paulo State serve as significant water sources due to their widespread occurrence in a substantial portion of Southeastern Brazil. In addition to São Paulo, the largest city in Latin America, other major urban centers in São Paulo State, such as Guarulhos and Campinas, also rely on the utilization of crystalline aquifers. The remarkable diversity in geotectonic contexts, lithology, geochemistry, and mineralogy observed in the crystalline basement of São Paulo State presents a significant opportunity to advance our quantitative understanding of rock–water interaction processes and their impact on groundwater hydrochemistry. Investigating these factors can provide valuable insights into the complex dynamics between rock and water, ultimately enhancing our knowledge of groundwater quality in the region. However, to date, a comprehensive study characterizing and modeling the hydrochemical evolution of crystalline aquifers in São Paulo State has not been undertaken. Therefore, this study has two main objectives. First, we aim to enhance our understanding of the mechanisms involved in the quantitative evaluation of hydrochemical evolution resulting from rock–water interactions. To achieve this, it is crucial to examine the underlying mechanisms and variables that influence the water quality of crystalline aquifers. Second, our objective is to develop a reliable model capable of accurately predicting the extent of rock–water interaction.

Materials and methods

Study area and regional geology

The study area is situated in the Crystalline Basement of the State of São Paulo, located in southeastern Brazil (Fig. 1). The rocks of the crystalline basement that

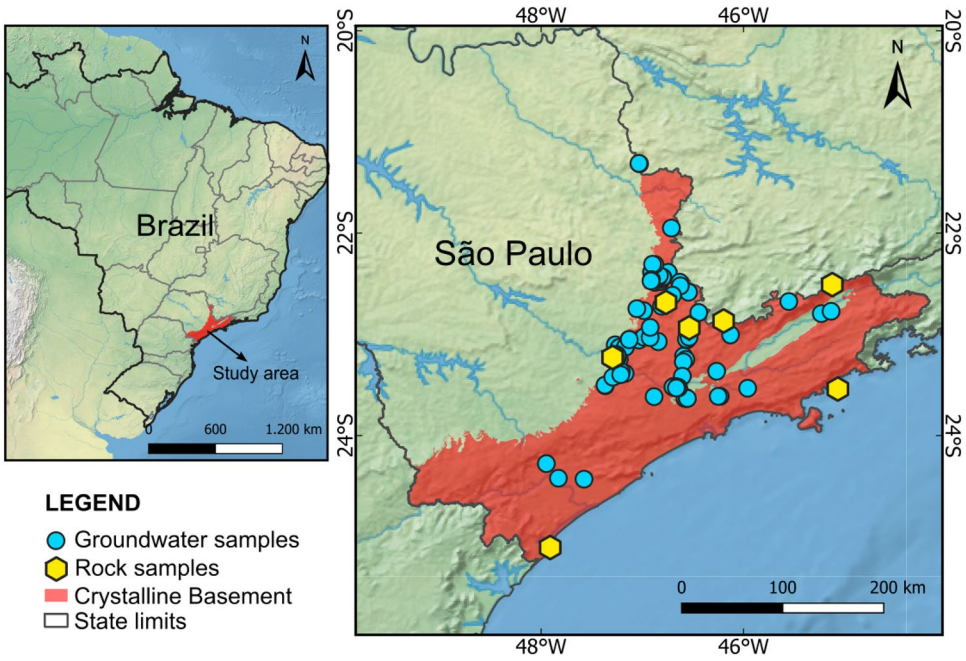

Fig. 1 The location of the compiled groundwater samples and of the region where the geochemistry of rock is available

occupies about 30% of the area of the State of São Paulo in its eastern region.

The focus of this study will be on the Mantiqueira Province as most of the samples are located within this unit. The Mantiqueira Province (Almeida et al. 1981) constitutes a complex Brazilian orogenic system (Fuck et al. 2008) that extends parallel to the east coast of Brazil in an approximate northeast direction. It stretches from southern Uruguay to southern Bahia, covering a length of over 3000 km (Heilbron et al. 2004). The province is delimited by the São Francisco, Tocantins, and Paraná provinces, as well as the basins of the East Continental Margin Province (Hasui 2010). It is compartmentalized into three main segments and five distinct orogens, as described by Heilbron et al. (2004): (a) the northern segment, which includes the Araçuaí Orogen; (b) the central segment, comprising the southern portion of the Brasília Orogen, and the Ribeira and Apiaí orogens; and (c) the southern segment, encompassing the Dom Feliciano and São Gabriel orogens.

Stratigraphically, the Mantiqueira Province can be divided into Archean and Paleoproterozoic basement rocks, metasedimentary sequences deposited in Paleoproterozoic to Mesoproterozoic intracontinental basins, Neoproterozoic metasedimentary and metavulcanosedimentary sequences, as well as Neoproterozoic granites and Neoproterozoic covers. The metamorphic grade recorded in the lands of the Mantiqueira Province ranges from greenschist facies to granulite facies (Heilbron et al. 2004).

Data collection and exploratory analysis

We analyzed a comprehensive dataset comprising 96 hydrochemical records extracted from six previously conducted studies carried out in the crystalline basement of São Paulo State, Southeastern Brazil. The sources of these data include Kiang et al. (2003), Iritani et al. (2011), DAEE (2011), Ezaki et al. (2014), Martins et al. (2018), and Teramoto et al. (2019).

The selection of data prioritized samples from the crystalline basement with plutonic or hypabyssal magmatic rocks, as well as rocks subjected to metamorphism in amphibolite facies or higher. Aquifers composed of metasedimentary/metabasic rocks with low metamorphic grade were excluded from the dataset. This ensured that the analyzed aquifers were predominantly composed of quartz, potassic feldspars, plagioclases, biotite, and amphibole. Additionally, we compiled available geochemical data to assess the compatibility of groundwater with the interacting rock. The locations of the sampled groundwater are depicted in Fig. 1, and the complete dataset is presented in Table S1 of the Supplementary Materials.

To setting the diverse geochemistry of rocks found in the crystalline basement of São Paulo, we compiled X-ray diffraction analyses from various rock samples published in previous works. The data sources include Spinelli and Barros (2009), Oliveira et al. (2008), Janasi et al. (2009), Sobrinho et al. (2011), Melo and Oliveira (2013), Duffles et al. (2013), and Toledo et al. (2018).

To conduct an initial assessment of compositional variations in the water samples, we performed hydrochemical typology and calculated the saturation index of the dissolved phase in groundwater. Additionally, we constructed a Cox Diagram to explore the distinct geochemistry of the rocks. Where both groundwater and rock analyses were conducted within the same aquifer, we endeavored to establish a correlation between them, seeking to identify any connections or relationships.

Geochemical conceptual model

We assume that the natural hydrochemistry of crystalline aquifers is governed by chemical interactions with the modal mineralogy of rocks. Consequently, the rock–water interaction is controlled by the dissolution of K-feldspar, plagioclase, pyroxenes, amphiboles, and biotite. Na^+, K^+, Ca^{2+}, Mg^{2+}, and HCO_3^- are assumed to be ions released into the water, while Cl^-, SO_4^{2-}, and NO_3^- are presumed to be derived from anthropogenic contamination.

Potassium feldspars (orthoclase and microcline) represent abundant mineral phases in granites and gneisses. The hydrolysis of potassium feldspars is responsible for the release of potassium into the water, as described in Eq. 1 (Appelo and Postma 2004)

$$2KAlSi_3O_8 + 2CO_2 + 11H_2O \rightarrow Al_2Si_2O_5(OH)_4 + 2K^+ + 2HCO_3^- + 4Si(OH)_4. \quad (1)$$

Plagioclases are significant mineral phases found in granitic/gneissic rocks, especially those of the tonalite and granodiorite types. The hydrolysis reactions of the terminal members of the plagioclase series, anorthite and albite, are presented in Eqs. 2 and 3, respectively (Appelo and Postma 2004)

$$CaAlSi_3O_8 + 2CO_2 + 3H_2O \rightarrow Al_2Si_2O_5(OH)_4 + Ca^{2+} + 2HCO_3^- + 4Si(OH)_4 \quad (2)$$

$$2NaAlSi_3O_8 + 2CO_2 + 11H_2O \rightarrow Al_2Si_2O_5(OH)_4 + 2Na^+ + 2HCO_3^- + 4Si(OH)_4. \quad (3)$$

Although amphiboles typically constitute a small percentage of granitoids (< 5%), these minerals can have a significant impact on groundwater composition due to their reactivity. Given the mineralogical composition of the examined rocks, it is likely that hornblende hydrolysis is the dominant source of magnesium in the water, as outlined in Eq. 4 (Helms et al. 1987)

$$Na_{0,5}Ca_2\left(Fe_{1,3}Mg_{2,6}Al_{1,1}\right)\left(Al_{1,6}Si_{6,4}\right)O_2 + 15H^+ + H_2O \rightarrow 0,5Na + 2Ca^{2+} + 2,6Mg^{2+} + 1,3Fe^{2+} + 2,7Al(OH)_2^+ + 6,4H_4SiO_4(aq). \quad (4)$$

In the case of an open system with respect to CO_2, which is expected to be true for fissured crystalline rocks, the pH is buffered by high PCO_2 levels, and HCO_3^- serves as the main anion produced by silicate hydrolysis, as demonstrated in Eqs. 1–3. We interpret the variations in major cations and HCO_3^- as distinct stages of rock–water interaction, forming a continuum reflecting the extent of reaction with the rock.

Kaolinite is widely acknowledged as the primary mineral phase resulting from the weathering of crystalline rocks, such as granite and gneiss, in tropical and subtropical climates (Eqs. 1–4) (e.g., Jeong 2000; Gurumurthy et al. 2012; Liu et al. 2016; Fuoco et al. 2022).

Geochemical simulation

To assess the extent of rock–water interaction, we categorized certain samples into geological groups and ranked them based on the concentrations of major cations and anions. All numerical geochemical simulations in our study were performed using Geochemist's Workbench 10.0 (GWB 10) software (Bethke and Yeakel 2018).

Speciation calculations were conducted using the Espec8 program within GWB 10 to determine the saturation state with respect to dissolved minerals. The saturation index (SI) of a specific mineral is obtained by dividing the chemical activities of the dissolved ions (ion activity product, IAP) by their solubility product (Ksp), as described in Eq. 5

$$SI = log_{10}\left(\frac{IAP}{K_{sp}}\right). \quad (5)$$

When the saturation index (SI) is lower than 0, the solution is unsaturated with respect to the evaluated mineral. An SI equal to 0 indicates that the solution is saturated with respect to the evaluated mineral. In the case of SI > 0, the mineral phase is supersaturated, leading to the precipitation of the mineral phase.

The reaction paths related to rock–water interaction was performed following the procedures described by Teramoto et al. (2019). The simulation of water composition variations as a function of rock–water interaction was conducted using the React program within GWB 10 and thermodynamic database thermo.tdat. These simulations aimed to reproduce changes in the chemical composition of water as water–rock interaction intensifies. Additionally,

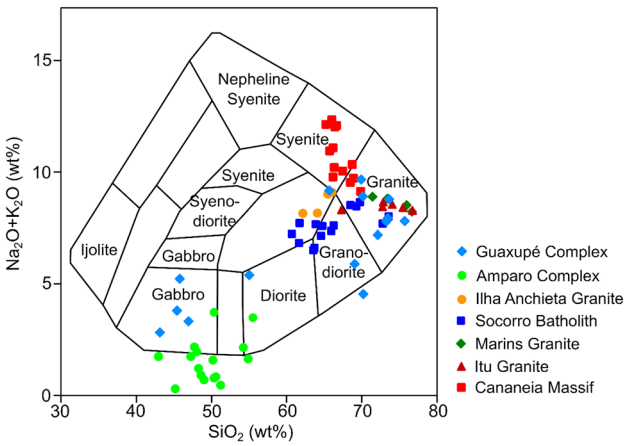

Fig. 2 Cox diagram illustrating the percentage of $Na_2O + K_2O$ plotted against SiO_2 in rock samples from selected lithostratigraphic units of the Crystalline Basement in São Paulo State. The diagram highlights the distinctiveness of rock geochemistry based on data acquired from literature sources

the simulations provided estimates of the mass balance of chemical species released into the water and the mass of secondary minerals produced from this interaction. Some reference samples were selected as criteria for adjusting the reacted mineralogy.

The initial solution was assumed to be pure water, with an average concentration of Cl^-, SO_4^{2-}, NO_3^-, and K^+ based on the reference samples. The selection of mineral phases for reference was based on the geological context of the water sources, and the masses of each reacted phase were manually adjusted. Since the GWB database did not include calcio-magnesian hornblende, we used tremolite as a proxy for magnesian amphibole. To enable the precipitation of supersaturated mineral phases, we activated the precipitation function in GWB. The resulting precipitated mineralogy was also calculated.

Results

Geochemistry of rocks

The geochemistry of the Precambrian basement exhibits a wide range of diversity, which aligns with its genetic context. Metamorphic rocks found in amphibolite and granulite facies include ortho- and para-derived gneiss, migmatites, granulites, and amphibolites. Additionally, there are scattered occurrences of sin- or post-orogenic granites, predominantly classified as monzogranite and syenogranite according to the QAP classification. The lithological diversity reflects the varied geochemistry of the rocks, as illustrated in Fig. 2. The samples of Amparo Complex (Oliveira et al. 2008) fall within gabbro field, since these rocks are derived from the metamorphism of tholeiitic basalts. The samples from the Amparo Complex (Oliveira et al. 2008) fall within the gabbro field, as these rocks originate from the metamorphism of tholeiitic basalts. The geochemistry of the Guaxupé Complex exhibits broad variation (Melo and Oliveira 2013), encompassing the paleosome of migmatites composed of tholeiitic basaltic orthogranulite, as well as the neosome formed through partial melting. The neosome exhibits a calc-alkaline composition, ranging from granitic to tonalitic, with high SiO_2 content. Additionally, samples from charnockite intrusions are also present.

Regarding the geochemistry of the rocks, our study focused on the major metallic elements that comprise the modal mineralogy of granitoids and gneiss, namely potassium, sodium, calcium, and magnesium. Generally, the granitoids exhibit a composition range from diorite to syenite, as shown in Fig. 2. The dominant element is K_2O (> 4.5 wt%), followed by Na_2O (0.28–7.11 wt%), CaO (0.05–4.22 wt%), and MgO (with average values below 0.5 wt%) (e.g., Janasi et al. 2009; Spinelli and Barros Gomes 2009; Duffles et al. 2013; Toledo et al. 2018). However, there are some rock formations that deviate from the typical granitoid composition. For instance, the Amparo Complex, which spans a large area in São Paulo State, is derived from the metamorphism of tholeiitic basalts. The average content of CaO, MgO, Na_2O, and K_2O in this complex is 10.66%, 11.89%, 1.24%, and 0.35% wt, respectively (Oliveira et al. 2008). Similarly, in the case of the paleosome of migmatites within the Guaxupé Complex, the average composition of CaO, MgO, Na_2O, and K_2O is 11.37%, 9.88%, 1.87%, and 0.85% wt, respectively (Melo and Oliveira 2013).

Characterization of evaluated samples

As illustrated in Eqs. 1–3, bicarbonate is the predominant anion resulting from rock–water interaction in an open system with respect to CO_2. Consequently, all water samples in our study are classified as either Ca–Mg–HCO_3 or Na–HCO_3 types, as depicted in Fig. 3. Three samples deviate from this classification and are categorized as Na-SO_4 types, indicating anthropogenic influence. The pH values of the water samples are consistently close to neutral, and the electrical conductivity (EC) exhibits a wide range of variation, spanning from 28 to 1,121 µS/cm.

The relationship between Electrical Conductivity (EC) and Total Dissolved Solids (TDS) is well established, with the former often used as an indicator for estimating the latter. By plotting the TDS values against the corresponding EC data (Fig. 4), we observed a linear relationship between the two parameters, which aligns with expectations. Through linear regression analysis with the intercept constrained at EC = 0 and TDS = 0, we determined that TDS can be

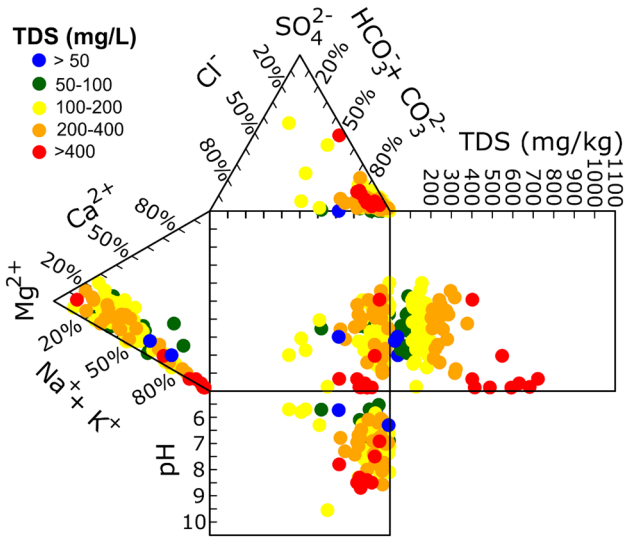

Fig. 3 Groundwater samples projected on the Durov diagram. The evaluated samples were classified into five distinct groups, according to TDS values

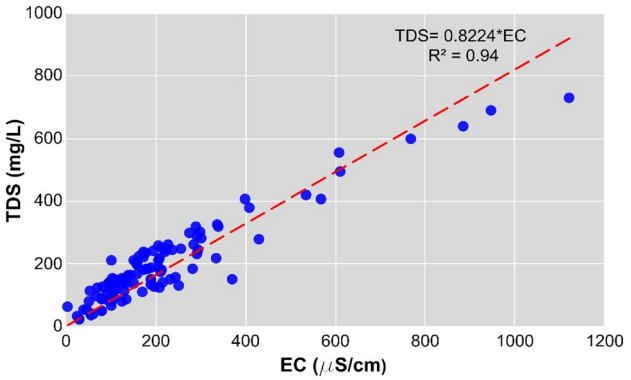

Fig. 4 Scatterplot of TDS versus EC values as a linear model

estimated by multiplying EC by 0.82 in crystalline aquifers in the studied area.

To assess the formation of authigenic minerals resulting from rock–water interaction, we constructed a stability diagram focusing on Ca-rich and Na-rich silicates. However, due to missing data on SiO_2 and Al^{3+} concentrations for some samples, they were not included in the diagram. Figure 5 illustrates that the majority of samples are located within the kaolinite field, indicating the prevalence of kaolinite formation. However, a few samples are classified under gibbsite and montmorillonite categories. It is worth noting that the samples falling within the montmorillonite field are characterized by high TDS values, suggesting a significant level of interaction with the rocks.

Geochemical simulation

To gain insights into the hydrochemical evolution of groundwater resulting from rock interaction in crystalline aquifers in São Paulo, we examined two theoretical endmembers: the Ca–Mg–HCO_3 and Na–HCO_3 types. In the first set of simulations, we focused on samples from the Amparo Complex, which consists of metamafic and amphibolites from the Amparo and Itapira complexes. For the second set of simulations, we chose samples representing sodium-rich rocks and those with an alkaline affinity. The quantities of precipitated kaolinite and quartz per liter of water are presented in Table 1, providing valuable information on mineral precipitation during rock–water interaction.

Figures 6 and 7 depict the Stiff diagrams comparing the results of the first and second sets of simulations, respectively, highlighting their similarities. The plagioclase series encompasses various intermediate types, spanning from predominantly calcium-based compositions (anorthite) to predominantly sodium-based compositions (albite). To replicate plagioclases with varying proportions of calcium and sodium in their compositions, we employed variable masses of anorthite and albite as the interacting minerals with water. Dissolved CO_2 values were adjusted to represent different PCO_2 conditions in the studied aquifers, resulting in hydrogen concentrations and alkalinities that closely resembled the observed values.

Figure 8 illustrates the evolution of CE, pH, TDS, HCO_3^- concentration, and the masses of precipitated kaolinite and quartz as a function of the reacted mass of rock (sum of reacted minerals). The figure shows that, for most of the presented parameters, there is a linear increase as the mass of reacted minerals increases. However, the pH exhibits a non-linear increase followed by a gradual rise, indicating the buffering effect of high PCO_2. This behavior reflects the system's ability to maintain pH within a certain range despite variations in the reacted mineral mass.

Due to the buffering effect caused by high PCO_2, water exhibits elevated concentrations of CO_2, which undergo hydrolysis to form HCO_3^- during interactions with rock. Taking this into consideration, we calculated an increase in HCO_3^- concentration corresponding to the reacted rock (Fig. 8). As depicted in the figure, the HCO_3^- concentration shows a linear increase in relation to the equivalent mass of the reacted rock.

Based on the linear correlation between HCO_3^- concentration and the mass of reacted minerals, we developed two linear equations for predicting the theoretical mass of reacted rock for the Ca–Mg–HCO_3 type (Eq. 6) and the Na–HCO3 type (Eq. 7). The distinction between these equations lies in the proportion of reacted amphibole, as these mineral lacks alumina

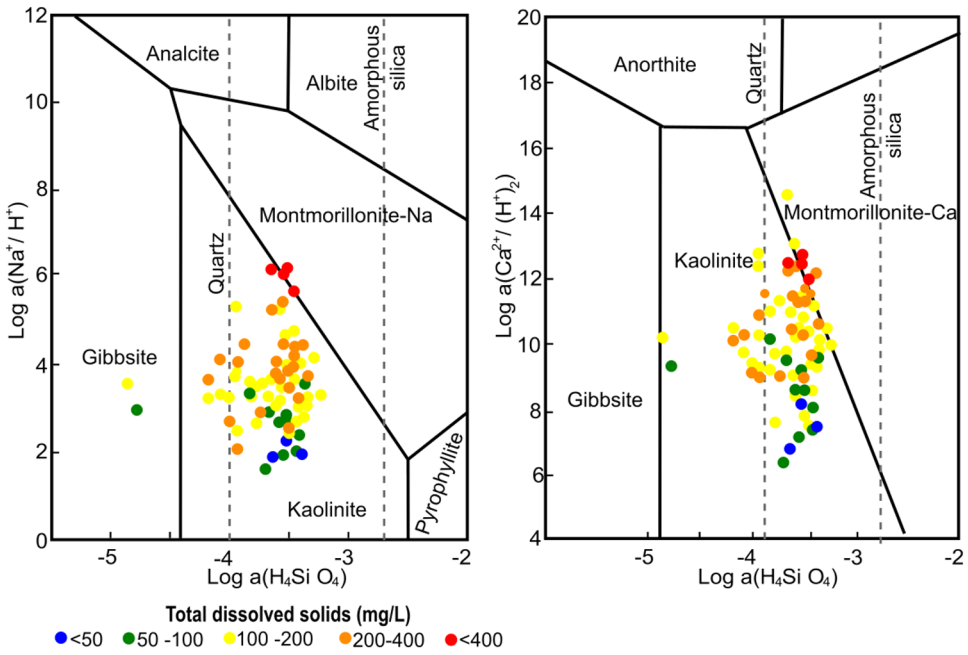

Fig. 5 Stability diagram regarding aluminum silicate minerals

Table 1 Mass of precipitated minerals calculated by simulations per liter of groundwater

Group	Mass of kaolinite precipitated (g)	Mass of quartz precipitated (g)
Amparo complex	0.1562	0.07988
Sodium-rich rock	0.2526	0.195

$$M_{interacted\ rock} = 0.002 \cdot HCO_3^- - 0.0408 \quad (6)$$

$$M_{interacted\ rock} = 0.0032 \cdot HCO_3^- - 0.0647. \quad (7)$$

Discussion

Our analysis was based on previously published works. Figure 1 illustrates a significant data gap in the southern portion of the study area, which limits our analysis in that region. The concentration of samples in specific regions introduces a potential bias into our analyses; however, we have confidence in the representativeness of our samples. They were collected from the principal lithostratigraphic groups encompassing the crystalline basement of the State of São Paulo.

During the hydrochemical characterization, we observed that all groundwater samples exhibited variations between the Ca, Mg–HCO_3 and Na–CO_3 types, as depicted in Fig. 3. This is likely due to the high annual precipitation in the studied area (> 1200 mm/year) and the subsequent leaching process. Most samples fall within the kaolinite and gibbsite fields, as shown in Fig. 5. These samples align along two reaction paths: one composed of orthogneisses from the Amparo Complex and the other involving sodium-rich rocks. To simulate the rock–water interaction within the Amparo Complex, we utilized amphiboles and calcium-rich plagioclases as reactant phases (Fig. 6). Conversely, to replicate the evolution of Na-HCO_3 types, the presence of sodium-rich plagioclase alone was sufficient (Fig. 7). In our simulations, the secondary mineralogy resulting from the dissolution of primary silicates consists exclusively of quartz and kaolinite (Table 1).

In addition to rock mineralogy, the climatic and hydrological conditions also exert an influence on rock–water interaction. Therefore, by conducting a comprehensive analysis of our study along with previous research that employed similar methodologies, we significantly advance the current understanding of the mechanisms that govern rock–water interaction in crystalline aquifers. Despite the recent publication of several relevant works deducing the mechanisms controlling water quality in crystalline rocks (e.g., Cho and Choo 2019; Cuccuru et al. 2020; Kumar and Kumar 2020; Abbas et al. 2021; Mao et al. 2022; Kouser et al. 2022; Ghalit et al. 2023), only a few of them (e.g., Fuoco et al. 2022; Manu et al. 2023) have utilized geochemical modeling to reproduce the reaction paths of rock–water interaction, enabling direct comparisons with our results.

When comparing our findings with previous studies that utilized similar modeling approaches (Fuoco et al. 2022; Manu et al. 2023), certain similarities arise, particularly in recognizing the significance of plagioclases as a key mineral group influencing hydrochemistry. From this perspective,

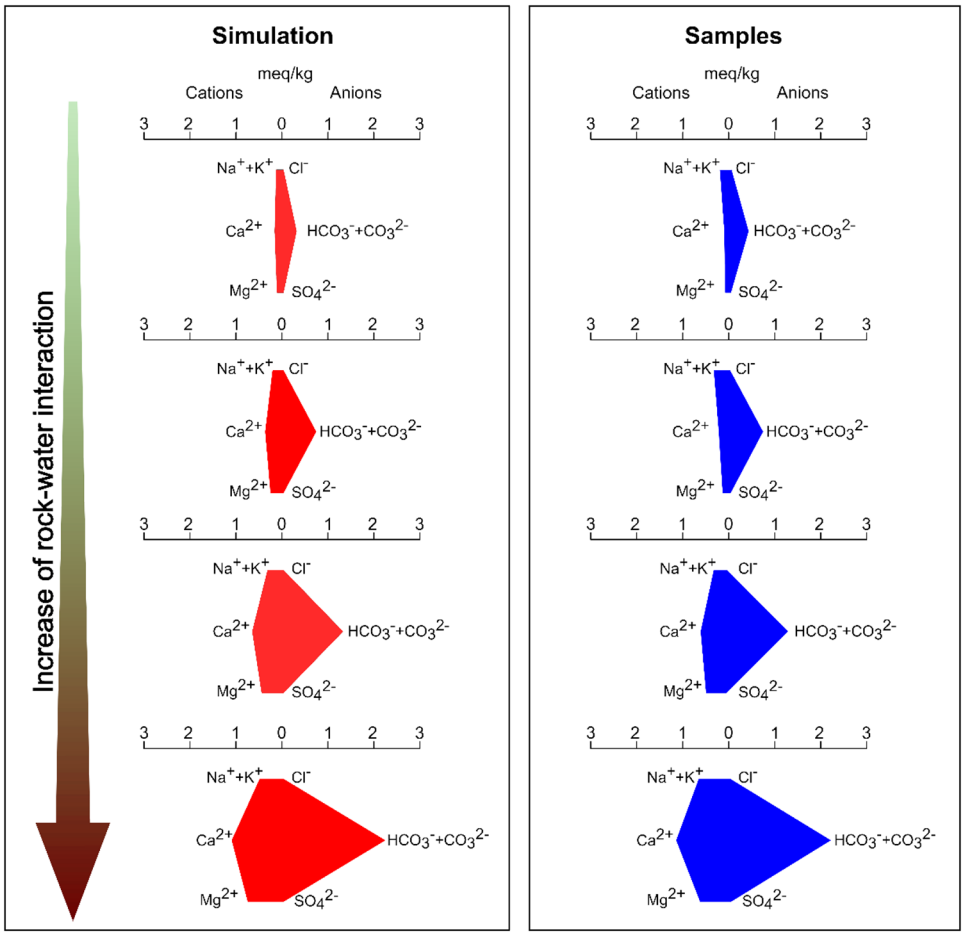

Fig. 6 Comparison of stiff diagram of simulated solution with distinct stages of rock–water interaction and data from Amparo complex samples

the concentrations of Na^+ and Ca^{2+} in groundwater can be predominantly influenced by the Na/Ca ratio in the reacted plagioclases. However, it is important to exercise caution when interpreting this statement, as the dissolution of plagioclases, as established by Stober and Bucher (1999), is notably incongruent. This means that while Ca is released into the groundwater, Na remains relatively unaffected within the crystal structure. Consequently, the proportions of reactive albite and anorthite adjusted in geochemical simulations may not accurately reflect the true composition of plagioclases.

In contrast to our findings, Fuoco et al. (2022) demonstrated in their geochemical simulations that biotite plays a significant role as the second most important reacted mineral, releasing magnesium into the groundwater. The use of biotite as a source of Mg^{2+} in crystalline aquifers is supported by several studies (e.g., Soulsby et al. 1998; Elango 2007; Jeong 2001; Venkatramanan et al. 2016), considering its abundance and reactivity. The average concentrations of Na^+, K^+, Ca^{2+}, and Mg^{2+} are 3.48 mmol/L, 0.056 mmol/L, 2.50 mmol/L, and 0.94 mmol/L, respectively. Thus, our samples display a relatively high proportion of magnesium, comparable to that of calcium and sodium, while showing a significantly lower concentration of potassium. This challenges the notion of biotite being the primary source of magnesium. Based on our model, amphiboles appear to be a more suitable candidate as the main source of magnesium.

According to the simulations by Fuoco et al. (2022), K-feldspar is postulated as the third most important mineral contributing to water quality. Since K-feldspar is one of the most abundant minerals in granitoids and gneiss, it is theoretically expected to have a significant impact on the hydrochemistry of crystalline aquifers. However, during our simulations, we observed that the contribution of K-feldspar to the hydrochemistry of crystalline aquifers is minimal, despite its abundance in granite/gneiss. This is indicated by the low activity of K^+ in almost all samples. We ruled out the possibility of potassium-rich clays, such as montmorillonite and illite, precipitating due to their low saturation indices. The preferential dissolution of plagioclases over K-feldspar can be attributed to the low reactivity of the latter mineral, with dissolution rates at least two-to-three orders of magnitude lower than those of plagioclases (e.g., White et al. 2001; Kampman et al. 2009; Zhu 2005).

In some locations where both the rock and geochemistry data were available, a comparative evaluation was possible.

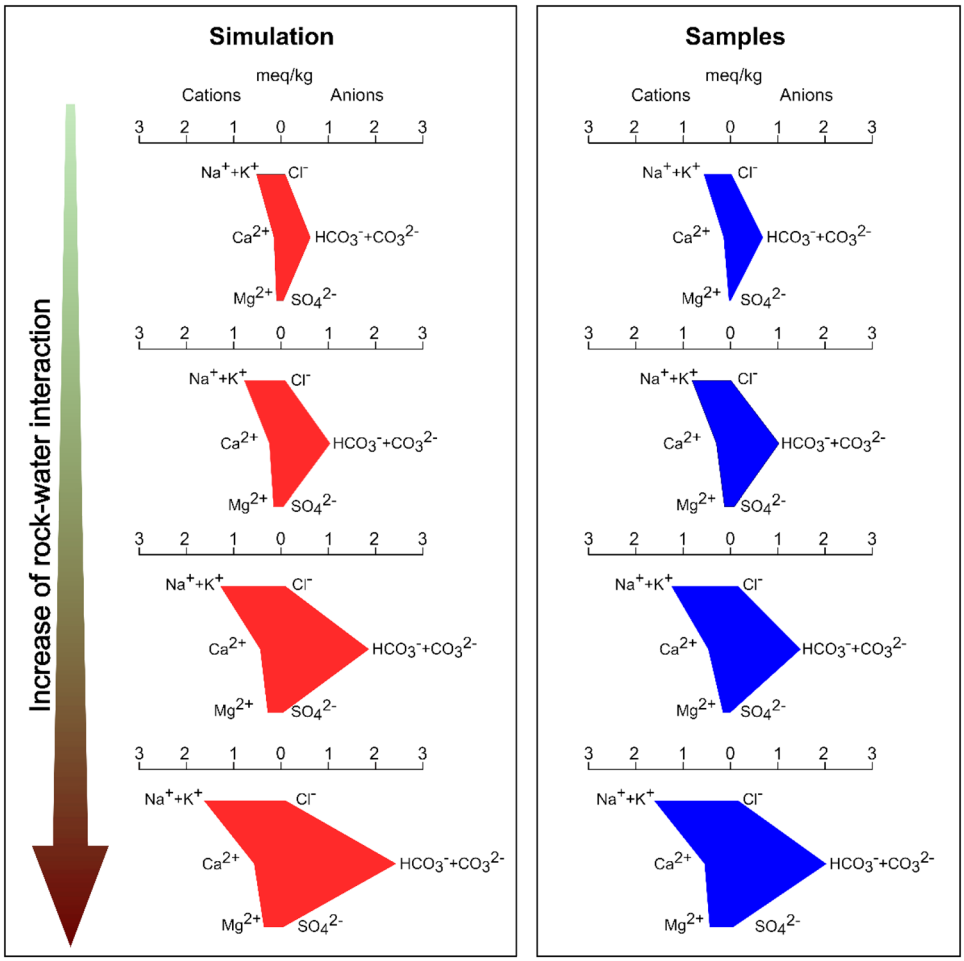

Fig. 7 Comparison of stiff diagram of simulated solution with distinct stages of rock–water interaction and data of sodium-rich samples

We note that groundwater samples collected at the occurrence of Amparo and Guaxupé Complex in the north portion of studied area, the concentration of calcium and magnesium is high, agreeing with rock geochemistry. On the other hand, in the locations markedly by occurrence of granitoids with composition varying between syenogranite and granodiorite, the sodium comprises the most important dissolved cation, with minor but important concentration of calcium and magnesium. In this case, our study reveals a discrepancy between groundwater and rock compositions, highlighting the need for a more nuanced interpretation.

As rock–water interaction is the primary mechanism influencing the water quality of crystalline aquifers, various metrics have been proposed to measure the extent of these processes. Our research demonstrates the suitability of HCO_3^- as a proxy for quantifying the extent of rock–water interaction, as this anion is exclusively generated through silicate hydrolysis in the studied area. However, it is important to note that this holds true under specific conditions, particularly in an open system with respect to CO_2, where the pH remains close to neutral and there is no carbonate precipitation or another external source of bicarbonate (e.g., calcite).

Conclusions

Through the compilation of hydrochemical data from groundwater in Precambrian crystalline rocks and the application of geochemical modeling, we have gained valuable insights into the primary mechanisms governing the chemical composition of these waters in the Southeast region of São Paulo State, Brazil. In our approach, we employed a reacted mineralogy adjustment in numerical simulations to accurately reproduce the two main hydrochemical evolution trends.

Our simulations revealed that the groundwater in crystalline aquifers in São Paulo consists of Na–HCO_3, Ca–Mg–HCO_3, or intermediate hydrochemical types. These types can be attributed to two distinct evolutionary trends in hydrochemistry. The Ca–Mg–HCO_3 types can be linked to the dissolution of amphiboles and plagioclases, while the sodium bicarbonate type can be reproduced by

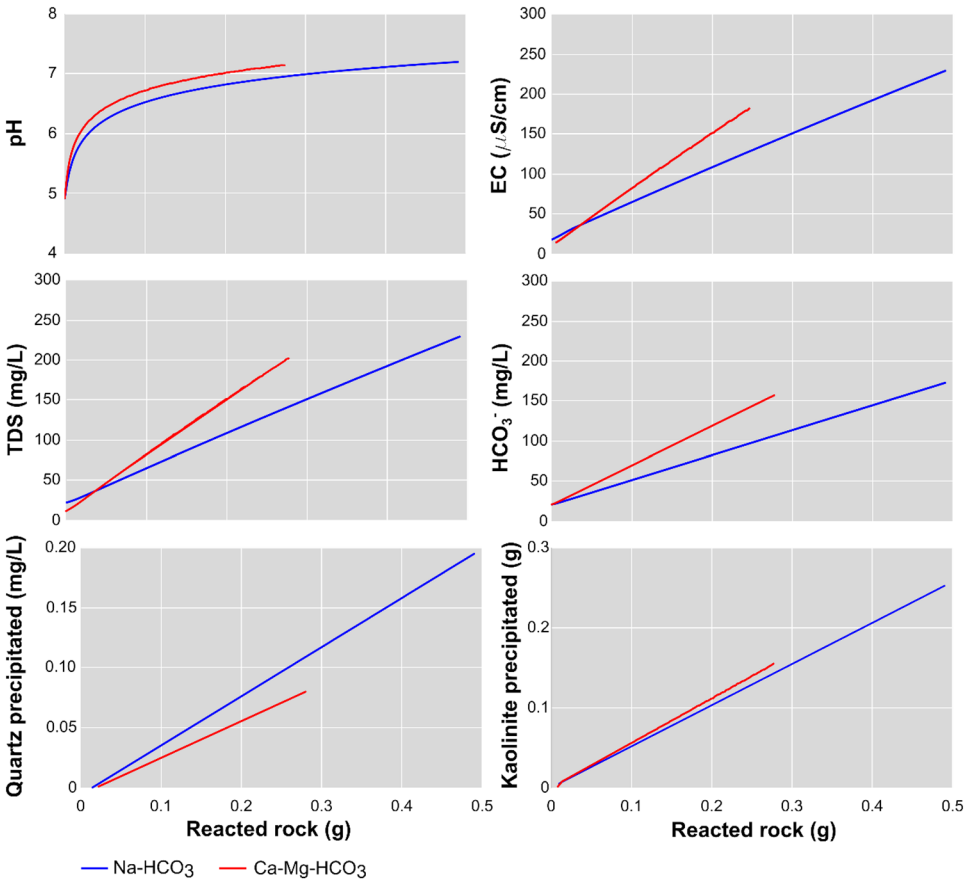

Fig. 8 Variation of pH, CE, TDS, HCO_3^-, and the amount of precipitated quartz and kaolinite as a function of the reacted rock (the sum of all dissolved minerals)

the dissolution of sodium-rich plagioclases. Consequently, in the studied area, the rock–water interaction can be simplified as involving the hydrolysis of plagioclase and amphiboles, leading to the precipitation of secondary mineralogy, such as kaolinite and quartz.

It is worth noting that despite the abundance of K-feldspar in the granitoids and its high percentage in the rocks, the concentration of K^+ in groundwater is very limited. While our results align with other studies that have reproduced the hydrochemical evolution resulting from rock–water interaction in crystalline aquifers, it is important to recognize that important features can vary significantly, and models should be applied with caution, considering the specificity of each site.

Another significant finding is that contrary to common belief, the hydrochemistry of the evaluated samples does not mimic the mineralogy or geochemistry of the granitic/gneiss rocks. Instead, the dissolved cations in groundwater mainly originate from unstable and reactive minerals, primarily represented by amphiboles and plagioclases. Finally, our simulations theoretically demonstrate that HCO_3^- can be utilized as a parameter to measure the extent of rock–water interaction in the studied area, as it is the main species produced through silicate hydrolysis under an open system with respect to CO_2.

Supplementary Information The online version contains supplementary material available at https://doi.org/10.1007/s40899-023-00946-8.

Acknowledgements The authors would like to thank the Fundação Para o Desenvolvimento da UNESP (FUNDUNESP) for granting research grants. The authors wish to extend their heartfelt appreciation to the two anonymous reviewers for their invaluable contributions through corrections and insightful suggestions.

Data availability The data are available upon reasonable request.

Declarations

Conflict of interest The authors declare that they have no known competing financial interests or personal relationships that could have appeared to influence the work reported in this paper.

References

Abbas M, Shen SL, Lyu HM, Zhou A, Rashid S (2021) Evaluation of the hydrochemistry of groundwater at Jhelum Basin, Punjab, Pakistan. Environ Earth Sci 80:1–17. https://doi.org/10.1007/s12665-021-09579-6

Ackerer J, Ranchoux C, Lucas Y, Viville D, Clément A, Fritz B, Leourge C, Schäfer G, Chabaux F (2021) Investigating the role of deep weathering in critical zone evolution by reactive transport modeling of the geochemical composition of deep fracture water.

Geochim Cosmochim Acta 312:257–278. https://doi.org/10.1016/jgca201801025
Adabanija MA, Afolabi OA, Lawal L (2020) The influence of bedrocks on groundwater chemistry in a crystalline basement complex of southwestern Nigeria. Environ Earth Sci 79:1–23. https://doi.org/10.1007/s12665-020-8822-y
Adimalla N, Venkatayogi SJEES (2017) Mechanism of fluoride enrichment in groundwater of hard rock aquifers in Medak, Telangana State, South India. Environ Earth Sci 76:1–10. https://doi.org/10.1007/s12665-016-6362-2
Akurugu BA, Obuobie E, Yidana SM, Stisen S, Seidenfaden IK, Chegbeleh LP (2022) Groundwater resources assessment in the Densu Basin: a review. J Hydrol: Regional Studies 40:101017. https://doi.org/10.1016/jejrh2022101017
Almeida FFM, Hasui Y, de Brito Neves BB, Fuck RA (1981) Brazilian structural provinces: an introduction. Earth Sci Rev 17:1–29. https://doi.org/10.1016/0012-8252(81)90003-9
Almeida S, Gomes L, Oliveira A, Carreira P (2022) Contributions for the understanding of the São Pedro do Sul (North of Portugal) geohydraulic and thermomineral system: hydrochemistry and stable isotopes studies. Geosciences 12:84. https://doi.org/10.3390/geosciences12020084
Alves FR, Gomes CB (2001) Ilha dos Búzios, Litoral Norte do Estado de São Paulo: aspectos geológicos e petrográficos. Geologia USP Série Científica 1:101–114. https://doi.org/10.5327/S1519-874X2001000100007
Apollaro C, Perri F, Le Pera E, Fuoco I, Critelli T (2019) Chemical and minero-petrographical changes on granulite rocks affected by weathering processes. Front Earth Sci 13:247–261. https://doi.org/10.1007/s11707-018-0745-5
Appelo CAJ, Postma D (2004) Geochemistry, groundwater and pollution. CRC Press
Banks D, Frengstad B (2006) Evolution of groundwater chemical composition by plagioclase hydrolysis in Norwegian anorthosites. Geochim Cosmochim Acta 70:1337–1355. https://doi.org/10.1016/jgca200511025
Benettin P, Bailey SW, Campbell JL, Green MB, Rinaldo A, Likens GE, McGuire KJ, Botter G (2015) Linking water age and solute dynamics in streamflow at the Hubbard Brook Experimental Forest, NH, USA. Water Resour Res 51:9256–9272. https://doi.org/10.1002/2015WR017552
Bethke CM, Farrell B, Yeakel S (2018) The geochemist's Workbench release 12, GWB essentials guide. Aqueous Solutions LLC Champaign, Illinois
Chae GT, Yun ST, Kwon MJ, Kim YS, Mayer B (2006) Batch dissolution of granite and biotite in water: Implication for fluorine geochemistry in groundwater. Geochemical J 40:95–102. https://doi.org/10.2343/geochemj4095
Chang HK, Teixeira A, Vidal AC (2003) Aspectos Hidrogeológicos e Hidroquímicos das regiões dos municípios de Mogi Mirim, Mogi Guaçu e Itapira no estado de São Paulo. Geociências 22:63–73
Cho BW, Choo CO (2019) Geochemical behavior of uranium and radon in groundwater of Jurassic granite area, Icheon. Middle Korea. Water 11:1278. https://doi.org/10.3390/w11061278
Choi H, Kim J, Shim BO, Kim DH (2020) Characterization of aquifer hydrochemistry from the operation of a shallow geothermal system. Water 12:1377. https://doi.org/10.3390/w12051377
Cuccuru S, Deluca F, Mongelli G, Oggiano G (2020) Granite-and andesite-hosted thermal water: geochemistry and environmental issues in northern Sardinia, Italy. Environ Earth Sci 79:257. https://doi.org/10.1007/s12665-020-09004-4
DAEE (2011) Bacias do Leste. Technical Report 62 pages
Duffles PAT, Trouw RAJ, Mendes JC, Gerdes A (2013) Marins Granite (MG/SP): petrography, geochemistry, geochronology, and geotectonic setting. Braz J Geol 43:487–500. https://doi.org/10.5327/Z2317-48892013000300006
Duranel A, Thompson JR, Burningham H, Durepaire P, Garambois S, Wyns R, Cubizolle H (2021) Modelling the hydrological interactions between a fissured granite aquifer and a valley mire in the Massif Central, France. Hydrol Earth Syst Sci 25:291–319
Elango L, Kannan R (2007) Rock–water interaction and its control on chemical composition of groundwater. Dev Environ Sci 5:229–243. https://doi.org/10.1016/S1474-8177(07)05011-5
Ezaki S, Iritani MA, Veiga C, Stradioto MR (2014) Hidroquímica dos aquíferos Tubarão e Cristalino na região de Indaiatuba-Rafard, Estado de São Paulo. Pesquisas Em Geociências 41:65–79. https://doi.org/10.22456/1807-980678036
Frengstad B, Banks D (2007) Universal controls on the evolution of groundwater chemistry in shallow crystalline rock aquifers: the evidence from empirical and theoretical studies. Groundwater in fractured rocks. CRC Press, Boca Raton, pp 291–306
Fuck RA, Neves BBB, Schobbehaus CF, Neves RA, Schobbenhaus C (2008) Rodinia descendants in south America. Precambr Res 160:108–126. https://doi.org/10.1016/jprecamres200704018
Fuoco I, Marini L, De Rosa R, Figoli A, Gabriele B, Apollaro C (2022) Use of reaction path modelling to investigate the evolution of water chemistry in shallow to deep crystalline aquifers with a special focus on fluoride. Sci Total Environ 830:154566. https://doi.org/10.1016/jscitotenv2022154566
Ganor J, Roueff E, Erel Y, Blum JD (2005) The dissolution kinetics of a granite and its minerals—implications for comparison between laboratory and field dissolution rates. Geochim Cosmochim Acta 69:607–621. https://doi.org/10.1016/jgca200408006
Ghalit M, Bouaissa M, Gharibi E, Taupin JD, Patris N (2023) Hydrogeochemical characteristics and isotopic tools used to identify the mineralization processes of bottled mineral water in Morocco. Geosciences 13:38. https://doi.org/10.3390/geosciences13020038
Godoy AM, Vieira OARP (2020) Geologia do maciço correas, sul do estado de São Paulo. Geosciences 39:297–316. https://doi.org/10.5016/geocienciasv39i214625
Gurumurthy GP, Balakrishna K, Riotte J, Braun JJ, Audry S, Shankar HU, Manjunatha BR (2012) Controls on intense silicate weathering in a tropical river, southwestern India. Chem Geol 300:61–69. https://doi.org/10.1016/jchemgeo201201016
Gustafson GUNNAR, Krásný J (1994) Crystalline rock aquifers: their occurrence, use and importance. Appl Hydrogeol 2:64–75. https://doi.org/10.1007/s100400050051
Hasui Y (2010) A grande colisão pré-cambriana do sudeste brasileiro e a estruturação regional. Geociências 2:141–169
Heilbron, M, Pedrosa-Soares, A C, Campos Neto, M D C, Silva, L D, Trouw, R A J, Janasi, V D A (2004) Província mantiqueira. Geologia do continente sul-americano: evolução da obra de Fernando Flávio Marques de Almeida, 203–235
Helms TS, McSween HY, Labotka TC, Jarosewich E (1987) Petrology of a Georgia Blue Ridge amphibolite unit with hornblende+ gedrite+ kyanite+ staurolite. Am Miner 72:1086–1096
Iritani MA, Yoshinaga-Pereira S, Ezali S, Oda GH, Ferreira LMR (2011) Caracterização hidroquímica das águas subterrâneas no Município de Itu (SP). Revista Do Instituto Geológico 32:1–26
Janasi VA, Vlach SRF, Costa Campos Neto M, Ulbrich HH (2009) Associated A-type subalkaline and high-K calc-alkaline granites in the Itu Granite Province, southeastern Brazil: petrological and tectonic significance. Can Mineral 47:1505–1526. https://doi.org/10.3749/canmin4761505
Jaunat J, Huneau F, Dupuy A, Celle-Jeanton H, Vergnaud-Ayraud V, Aquilina L, Labasque T, Le Coustumer P (2012) Hydrochemical data and groundwater dating to infer differential flowpaths through weathered profiles of a fractured aquifer. Appl Geochem 27:2053–2067. https://doi.org/10.1016/japgeochem201206009

Jeong GY (2000) The dependence of localized crystallization of halloysite and kaolinite on primary minerals in the weathering profile of granite. Clays Clay Miner 48:196–203. https://doi.org/10.1346/CCMN20000480205

Jeong CH (2001) Effect of land use and urbanization on hydrochemistry and contamination of groundwater from Taejon area. Korea J Hydrol 253:194–210. https://doi.org/10.1016/S0022-1694(01)00481-4

Ju Y, Ryu JH, Drake H, Im HS, Baik MH (2023) Long-term change in uranium migration processes in highly eroded granite, demonstrated by uranium series disequilibrium in fracture-filling materials. Appl Geochem 148:105530. https://doi.org/10.1016/japgeochem2022105530

Knauss KG, Wolery TJ (1986) Dependence of albite dissolution kinetics on pH and time at 25 °C and 70 °C. Geochim Cosmochim Acta 50:2481–2497. https://doi.org/10.1016/0016-7037(86)90031-1

Kouser B, Bala A, Verma O, Prashanth M, Khosla A, Pir RA (2022) Hydrochemistry for the assessment of groundwater quality in the Kathua region, Jammu and Kashmir, India. Appl Water Sci 12:143. https://doi.org/10.1007/s13201-022-01673-9

Kumar M, Das A, Das N, Goswami R, Singh UK (2016) Co-occurrence perspective of arsenic and fluoride in the groundwater of Diphu, Assam, Northeastern India. Chemosphere 150:227–238. https://doi.org/10.1016/jchemosphere201602019

Kumar P, Mahajan AK, Kumar A (2020) Groundwater geochemical facie: implications of rock–water interaction at the Chamba city (HP), northwest Himalaya, India. Environ Sci Pollut Res 27:9012–9026. https://doi.org/10.1007/s11356-019-07078-7

Lachassagne P, Dewandel B, Wyns R (2021) Hydrogeology of weathered crystalline/hard-rock aquifers—guidelines for the operational survey and management of their groundwater resources. Hydrogeol J 29:2561–2594. https://doi.org/10.1007/s10040-021-02339-7

Liu W, Liu C, Brantley SL, Xu Z, Zhao T, Liu T, Gu X (2016) Deep weathering along a granite ridgeline in a subtropical climate. Chem Geol 427:17–34. https://doi.org/10.1016/jchemgeo201602014

Machado R, Demange M (1994) Classificação estrutural e tectônica dos granitóides neoproterozóicos do Cinturão Paraíba do Sul no Estado do Rio de Janeiro. Boletim IG-USP Série Científica 25:81–96. https://doi.org/10.11606/issn2316-8986v25i0p81-96

Manu E, Lucia MD, Kühn M (2023) Water–Rock interactions driving groundwater composition in the pra basin (Ghana) identified by combinatorial inverse geochemical modelling. Minerals 13:899. https://doi.org/10.3390/min13070899

Mao X, Dong Y, He Y, Zhu D, Shi Z, Ye J (2022) The effect of granite fracture network on silica-enriched groundwater formation and geothermometers in low-temperature hydrothermal system. J Hydrol 609:127720. https://doi.org/10.1016/jjhydrol2022127720

Marçais J, Gauvain A, Labasque T, Abbott BW, Pinay G, Aquilina L, de Dreuzy JR (2018) Dating groundwater with dissolved silica and CFC concentrations in crystalline aquifers. Sci Total Environ 636:260–272. https://doi.org/10.1016/jscitotenv201804196

Martins FAG (2003) Contexto geológico e potencial mineral do granito Serra do Paratiú, Cananéia, Estado de São Paulo. Boletim Paranaense De Geociências 52:97–114

Martins VTDS, Pino DS, Bertolo R, Hirata R, Babinski M, Pacheco DF, Rios AP (2018) Who to blame for groundwater fluoride anomaly in São Paulo, Brazil? Hydrogeochemistry and isotopic evidence. Appl Geochem 90:25–38. https://doi.org/10.1016/japgeochem201712020

Melo RPD, Farias de Oliveira MA (2013) Geology and lithogeochemistry of migmatites, charnockites and granulites of the Guaxupe Complex, Sao Joao da Boa Vista region, Sao Paulo State, Brazil. Braz J Geol. https://doi.org/10.5327/Z2317-48892013000200005

Milesi V, Shock E, Seewald J, Trembath-Reichert E, Sylva SP, Huber JA, Lim DSS, German CR (2023) Multiple parameters enable deconvolution of water-rock reaction paths in low-temperature vent fluids of the Kama'ehuakanaloa (Lō'ihi) seamount. Geochim Cosmochim Acta 348:54–67. https://doi.org/10.1016/j.gca.2023.03.013

Mizuno T, Suzuki Y, Milodowski AE, Iwatsuki T (2023) Isotopic signals in fracture-filling calcite showing anaerobic oxidation of methane under freshwater conditions in a granitic basement. Appl Geochem 150:105571. https://doi.org/10.1016/japgeochem2023105571

Nagaraju A, Thejaswi A, Sun L (2016) Statistical analysis of high fluoride groundwater hydrochemistry in Southern India: Quality assessment and Implications for source of fluoride. Environ Eng Sci 33:471–477. https://doi.org/10.1089/ees20150511

Nakayama H, Yamasaki Y, Nakaya S (2022) Effect of hydrogeological structure on geogenic fluoride contamination of groundwater in granitic rock belt in Tanzania. J Hydrol 612:128026. https://doi.org/10.1016/jjhydrol2022128026

Négrel P (2006) Water–granite interaction: clues from strontium, neodymium and rare earth elements in soil and waters. Appl Geochem 21:1432–1454. https://doi.org/10.1016/japgeochem200604007

Ojok W, Wanasolo W, Wasswa J, Bolender J, Ntambi E (2021) Hydrochemistry and fluoride contamination in Ndali-Kasenda crater lakes, Albertine Graben: assessment based on multivariate statistical approach and human health risk. Groundw Sustain Dev 15:100650. https://doi.org/10.1016/jgsd2021100650

Oliveira MAF, Zanardo A, Lazarini AP, Silva AHM, Nardy AJR (2008) Caracterização petrográfica e geoquímica de rochas anfibolíticas e metamáficas associadas às Faixas Metamórficas Amparo e Itapira na região nordeste de São Paulo. Braz J Geol 34:393–400

Olofinlade WS, Daramola SO, Olabode OF (2018) Hydrochemical and statistical modeling of groundwater quality in two constrasting geological terrains of southwestern Nigeria. Model Earth Syst Environ 4:1405–1421. https://doi.org/10.1007/s40808-018-0486-

Pauwels H, Négrel P, Dewandel B, Perrin J, Mascré C, Roy S, Ahmed S (2015) Hydrochemical borehole logs characterizing fluoride contamination in a crystalline aquifer (Maheshwaram, India). J Hydrol 525:302–312. https://doi.org/10.1016/jjhydrol201503017

Pereira RM, Ávila CA, Moura CAV, Roig HL (2001) Geologia e geoquímica do granito Mendanha e do granitóide Marins e idade 207Pb/206Pb do Granito Mendanha, Faixa Ribeira, São Paulo. Geociências 20:37–48

Procházka V, Zachariáš J, Strnad L (2018) Model ages of fracture fillings and mineralogical and geochemical evidence for water-rock interaction in fractures in granite: The Melechov Massif, Czech Republic. Appl Geochem 95:124–138. https://doi.org/10.1016/japgeochem201805016

Rashid A, Farooqi A, Gao X, Zahir S, Noor S, Khattak JA (2020) Geochemical modeling, source apportionment, health risk exposure and control of higher fluoride in groundwater of sub-district Dargai Pakistan. Chemosphere 243:125409. https://doi.org/10.1016/jchemosphere2019125409

Roy A, Keesari T, Mohokar H, Pant D, Sinha UK, Mendhekar GN (2020) Geochemical evolution of groundwater in hard-rock aquifers of South India using statistical and modelling techniques. Hydrol Sci J 65:951–968. https://doi.org/10.1080/02626667201917089 14

Salazar-Naranjo AF, Vlach SRF (2018) On the crystallization conditions of the Neoproterozoic, high-K calc-alkaline, Bragança Paulista-type magmatism, southern Brasília Orogen, SE Brazil. Braz J Geol 48:631–650. https://doi.org/10.1590/2317-4889201820180033

Sanchez-Roa C, Saldi GD, Mitchell TM, Iacoviello F, Bailey J, Shearing PR, Oelkers EH, Meredth AP, Jones AP, Striolo A (2021) The role of fluid chemistry on permeability evolution in granite:

Applications to natural and anthropogenic systems. Earth Planet Sci Lett 553:116641. https://doi.org/10.1016/jepsl2020116641
Sobrinho JMA, Janas VA, Simonetti A, Heaman LM, Diniz HN (2011) The Ilha Anchieta Quartz Monzonite: the southernmost expression of ca 500 Ma post-collisional magmatism in the Ribeira Belt. An Acad Bras Ciênc 83:891–906
Soulsby C, Chen M, Ferrier RC, Helliwell RC, Jenkins A, Harriman R (1998) Hydrogeochemistry of shallow groundwater in an upland Scottish catchment. Hydrol Process 12:1111–1127
Spinelli FP, Gomes CB (2009) A ocorrência alcalina de Cananéia, litoral sul do estado de São Paulo: petrologia e geoquímica. Revista Brasileira De Geociências 39(2):305
Stillings LL, Drever JI, Brantley SL, Sun Y, Oxburgh R (1996) Rates of feldspar dissolution at pH 3–7 with 0–8 m M oxalic acid. Chem Geol 132:79–89. https://doi.org/10.1016/S0009-2541(96)00043-5
Stober I, Bucher K (1999) Deep groundwater in the crystalline basement of the Black Forest region. Appl Geochem 14:237–254. https://doi.org/10.1016/S0883-2927(98)00045-6
Stober I, Giovanoli F, Wiebe V, Bucher K (2022) Deep hydrochemical section through the Central Alps: evolution of deep water in the continental upper crust and solute acquisition during water–rock-interaction along the Sedrun section of the Gotthard Base Tunnel. Swiss J Geosci 115:9. https://doi.org/10.1186/s00015-022-00413-0
Stradioto MR, Teramoto EH, Chang HK (2020) Rock-solute reaction mass balance of water flowing within an aquifer system with geochemical stratification. Appl Geochem 123:104784. https://doi.org/10.1016/j.apgeochem.2020.104784
Sung KY, Yun ST, Park ME, Koh YK, Choi BY, Hutcheon I, Kim KH (2012) Reaction path modeling of hydrogeochemical evolution of groundwater in granitic bedrocks, South Korea. J Geochem Explor 118:90–97. https://doi.org/10.1016/jgexplo201205004
Sunkari ED, Abu M (2019) Hydrochemistry with special reference to fluoride contamination in groundwater of the Bongo District, Upper East Region, Ghana. Sustain Water Resour Manag 5:1803–1814. https://doi.org/10.1007/s40899-019-00335-0
Teramoto EH, Navarro J, Kiang CH (2019) Avaliação geoquímica das águas envasadas de aquíferos cristalinos no sul e sudeste do Brasil. Revista do Instituto Geológico 40: 53–67. https://doi.org/10.33958/revigv40i2647
Toledo BB, Janasi VDA, Silva LGRD (2018) SHRIMP U-Pb Geochronology of the Socorro Batholith and implications for the Neoproterozoic evolution in SE Brazil. Braz J Geol 48:761–782. https://doi.org/10.1590/2317-4889201820180040
Venkatramanan S, Chung SY, Kim TH, Kim BW, Selvam S (2016) Geostatistical techniques to evaluate groundwater contamination and its sources in Miryang City, Korea. Environ Earth Sci 75:1–14. https://doi.org/10.1007/s12665-016-5813-0
Wanner C, Bucher K, von Strandmann PAP, Waber HN, Pettke T (2017) On the use of Li isotopes as a proxy for water–rock interaction in fractured crystalline rocks: A case study from the Gotthard rail base tunnel. Geochim Cosmochim Acta 198:396–418. https://doi.org/10.1016/jgca201611003
Welch SA, Ullman WJ (1996) Feldspar dissolution in acidic and organic solutions: compositional and pH dependence of dissolution rate. Geochim Cosmochim Acta 60:2939–2948. https://doi.org/10.1016/0016-7037(96)00134-2
White AF, Bullen TD, Schulz MS, Blum AE, Huntington TG, Peters NE (2001) Differential rates of feldspar weathering in granitic regoliths. Geochim Cosmochim Acta 65:847–869. https://doi.org/10.1016/S0016-7037(00)00577-9
Yuguchi T, Izumino Y, Sasao E (2021) Genesis and development processes of fractures in granite: Petrographic indicators of hydrothermal alteration. PLoS ONE 16:e0251198. https://doi.org/10.1371/Jpone0251198
Zango MS, Anim-Gyampo M, Gibrilla A, Pelig-Ba KB, Okofo LB (2023) Groundwater recharge and dating in crystalline basement aquifers of Vea catchment: an integrated environmental tracers' approach. Sci Afr 19:e01505. https://doi.org/10.1016/jsciaf2022e01505
Zhang L, Lüttge A (2009) Theoretical approach to evaluating plagioclase dissolution mechanisms. Geochim Cosmochim Acta 73:2832–2849. https://doi.org/10.1016/jgca200902021
Zhu C (2005) In situ feldspar dissolution rates in an aquifer. Geochim Cosmochim Acta 69:1435–1453. https://doi.org/10.1016/jgca200409005
Zhu C, Rimstidt JD, Zhang Y, Kang J, Schott J, Yuan H (2020) Decoupling feldspar dissolution and precipitation rates at near-equilibrium with Si isotope tracers: implications for modeling silicate weathering. Geochim Cosmochim Acta 271:132–153. https://doi.org/10.1016/jgca201912024